Development 133, 4305-4314 (2006) doi:10.1242/dev.02604

LONGIFOLIA1 and *LONGIFOLIA2*, two homologous genes, regulate longitudinal cell elongation in *Arabidopsis*

Young Koung Lee[1,*], Gyung-Tae Kim[2,3,*], In-Jung Kim[4], Jeongmoo Park[1], Sang-Soo Kwak[5], Giltsu Choi[1,†] and Won-Il Chung[1,†]

Plants have diversified their leaf morphologies to adapt to diverse ecological niches. The molecular components responsible for regulating leaf morphology, however, have not been fully elucidated. By screening *Arabidopsis* activation-tagging lines, we identified a dominant mutant, which we designated *longifolia1-1D* (*lng1-1D*). *lng1-1D* plants were characterized by long petioles, narrow but extremely long leaf blades with serrated margins, elongated floral organs, and elongated siliques. The elongated leaves of the mutant were due to increased polar cell elongation rather than increased cell proliferation. Molecular characterization revealed that this phenotype was caused by overexpression of the novel gene *LNG1*, which was found to have a homolog, *LNG2*, in *Arabidopsis*. To further examine the role of the LNG genes, we characterized *lng1* and *lng2* loss-of-function mutant lines. In contrast to the elongated leaves of *lng1-1D* plants, the *lng1* and *lng2* mutants showed slightly decreased leaf length. Furthermore, the *lng1-3 lng2-1* double mutant showed further decreased leaf length associated with less longitudinal polar cell elongation. The leaf widths in *lng1-3 lng2-1* mutant plants were similar to those in wild type, implying that the role of *LNG1* and *LNG2* on polar cell elongation is similar to that of *ROTUNDIFOLIA3* (*ROT3*). However, analysis of a *lng1-3 lng2-1 rot3-1* triple mutant and of a *lng1-1D rot3-1* double mutant indicated that *LNG1* and *LNG2* promote longitudinal cell elongation independently of *ROT3*. Taken together, these findings indicate that *LNG1* and *LNG2* are new components that regulate leaf morphology by positively promoting longitudinal polar cell elongation independently of *ROT3* in *Arabidopsis*.

KEY WORDS: *Arabidopsis*, Polar cell elongation, Leaf development, *LONGIFOLIA*

INTRODUCTION

As sessile organisms, plants have had to adapt their growth and development to diverse habitats and ecological niches, in part by diversifying the shape, size, form and arrangement of their leaves. As leaf morphology is closely associated with the habitats and ecological niches in which a plant is able to grow, the potential benefits from genetically engineering leaf morphology are immense. In addition, the diversity in leaf morphology between closely related species or within a single species provides an excellent opportunity to investigate how a living form is shaped by the interplay of various genes, and how this interplay is modified during evolution.

Leaf morphogenesis is conceptually divided into three processes: leaf initiation, establishment of polarity and leaf expansion. During initiation, the leaf primordia are formed at the periphery of the shoot apical meristem (SAM). Polarity is established with regards to the three main axes: the proximodistal axis (also called the apicobasal axis, and herein referred to as the leaf-length direction); the dorsoventral axis (also called the adaxial-abaxial axis); and the left/right axis (also called the mediolateral axis, and herein referred to as the leaf-width direction). Subsequently, the leaves expand to their final shapes and sizes (Sinha, 1999; Bowman et al., 2002; Kim and Cho, 2006).

[1]Department of Biological Sciences, KAIST, Daejeon 305-701, Korea. [2]Division of Molecular Biotechnology, Dong-A University, Busan 604-714, Korea. [3]Environmental Biotechnology Research Center, Gyeongsang National University, Jinju 660-701, Korea. [4]Faculty of Biotechnology, College of Applied Life Sciences, Cheju National University, Jeju 690-756, Korea.[5]Laboratory of Environmental Biotechnology, Korea Research Institute of Bioscience and Biotechnology (KRIBB), 52 Eoen-dong, Yuseong-gu, Daejeon, 305-806, Korea.

*These authors contributed equally to this work
†Authors for correspondence (e-mail: gchoi@kaist.ac.kr; wichung@kaist.ac.kr)

Accepted 30 August 2006

The final shape and size of an adult leaf is modulated by leaf expansion, which is in turn dependent upon cell division and expansion. The importance of cell proliferation on leaf morphology can be observed in *Arabidopsis* transgenic lines expressing *cyclin-dependent kinase inhibitor 1* (*ICK1*) or *Kip-related protein 2* (*KRP2*), which inhibit leaf cell proliferation through interactions with CDKA1/cyclin complexes (Wang et al., 2000; Verkest et al., 2005). Overexpression of these genes has been associated with the development of small serrated leaves that have reduced cell numbers. However, although this suggests that general cell proliferation is crucial for the determination of leaf shape and size, changes in cell proliferation do not always result in altered leaf shapes. For example, overexpression of *ABP1* results in decreased cell proliferation but increased cell volume without gross changes in leaf morphology (Jones et al., 1998). Furthermore, studies have shown that increased cell numbers could be compensated for by decreases in cell size, or vice versa (Hemerley et al., 1995; De Veylder et al., 2001; Ullah et al., 2001; Tsukaya, 2003). In addition, other factors regulate leaf morphogenesis by affecting polarity-dependent cell proliferation. Recently, *ROTUNDIFOLIA4* (*ROT4*), which encodes a membrane-bound small peptide, was shown to inhibit cell proliferation in only the leaf-length direction in *Arabidopsis*. Conversely, it was also shown that ectopic expression of *ROT4* caused short leaves (Narita et al., 2004). Thus, both general and specific cell proliferation can affect leaf morphology.

Cell expansion also plays an important role in the leaf expansion required for the proper formation of a mature leaf. Genetic analyses have indicated that cell expansion is regulated independently in the leaf-length and leaf-width directions. Mutation of the *ANGUSTIFOLIA* (*AN*) gene, which encodes a C-terminal binding protein (CtBP) that is responsible for regulating the arrangement of microtubules in leaf cells, caused a defect in cell expansion in the leaf-width direction, resulting in narrower leaves (Kim et al., 2002).

By contrast, the mutation of *ROT3*, which encodes a P450 involved in brassinosteroid (BR) biosynthesis, decreased cell expansion in the leaf-length direction, resulting in shorter leaves (Kim et al., 1998). This finding of an association between *ROT3* and leaf expansion provided evidence that BR promotes cell expansion in the leaf-length direction (Kim et al., 1998; Kim et al., 1999; Kim et al., 2005). Similar findings were observed in other BR biosynthetic mutants, including *de-etiolated 2* (*det2*) and *dwarf4* (*dwf4*) – both of which show shortened leaves (Altmann, 1998; Fujioka et al., 1997; Li and Chory, 1997; Azpiroz et al., 1998; Choe et al., 1998). Other factors that affect cell expansion, including auxins and light, have also been found to regulate leaf morphology (Timpte et al., 1992; Qin et al., 1997; Franklin et al., 2003; Kozuka et al., 2005)

The different leaf morphologies observed in the various *Arabidopsis* ecotypes are likely to be determined by multiple factors. A genetic screen of leaf-shape mutants from 5770 M1 EMS-mutagenized *Arabidopsis* plants generated 94 complementation groups that showed altered leaf morphology (Berna et al., 1999). A quantitative trait loci (QTL) analysis using recombinant inbred Ler and Col-4 lines identified 21 loci that affect six different characteristics of the adult leaf (Perez-Perez et al., 2002). These previous studies suggest that leaf morphogenesis is a complex process requiring the interplay of many different genetic components. However, although many factors involved in leaf morphogenesis have been identified, other genetic components remain to be examined before the determination of leaf shape is fully understood. Here, we have screened *Arabidopsis* leaf-shape mutants in an effort to discover new genetic components and to report the identification of two new genetic components, *LONGIFOLIA1* (*LNG1*) and *LONGIFOLIA2* (*LNG2*), that are responsible for regulating leaf morphology by promoting cell expansion in the leaf-length direction in a *ROT3*-independent fashion.

MATERIALS AND METHODS

Plant materials and growth conditions

Arabidopsis thaliana plants (Col-0 ecotype background) were maintained in a greenhouse at 22-24°C with a 16 hour/8 hour light/dark cycle for general growth. Activation-tagged T-DNA insertion lines were generated by a dipping procedure (Clough and Bent, 1998), using *Agrobacterium* harboring the activation-tagging vector pSKI1015 (Weigel et al., 2000). The *lng1-1D* mutant plant was selected from herbicide (ammonium glufosinate, known as Basta)-resistant transgenic lines. Loss-of-function mutant alleles (*lng1-2*, *lng1-3*, *lng2-1* and *lng2-2*) were obtained from the SALK Institute Genomic Analysis Laboratory (salk_107002, salk_135585, salk_067658, salk_034645 and salk_130006, respectively). For generation of the *lng1 lng2* double homozygous mutant, homozygous *lng1* plants were crossed with homozygous *lng2* plants. Homozygous *lng1 lng2* double mutants were identified by PCR analysis from the F2 population using *LNG1*- and *LNG2*-specific primers (LBa1, 5′-TGG TTC ACG TAG TGG GCC ATC G-3′ and LBb1: 5′-GCG TGG ACC GCT TGC TGC AAC T-3′).

Expression analysis

For northern analysis, total RNA was extracted from 3-week-old seedlings using the RNeasy plant mini kit (Qiagen) and 20 μg total RNA was resolved from each sample by 1.2% agarose gel electrophoresis. The separated RNAs were transferred to a nylon membrane (Hybond-N; Amersham), and the filters were prehybridized for 1-2 hours at 42°C in 50% formamide, 5×SSPE, 5×Denhardt's solution, 0.1% SDS and 100 μg/ml denatured salmon sperm DNA. For hybridization, a ^{32}P-dCTP-labeled probe (described below) was added to the prehybridization buffer and the filter was hybridized overnight. Washes were performed twice at room temperature for 10 minutes in 2×SSC and 0.1% SDS, once at 65°C for 15 minutes in 1×SSC and 0.1% SDS, and twice at 65°C for 15 minutes in 0.1×SSC and 0.1% SDS. Results were analyzed with a scanning densitometer (Pharmacia), with adjustments being made for small differences in RNA loading. The probes were generated by RT-PCR from total RNA (described below) using specific primers (At5g15580 F, 5′-TTG GTT GCC CAC TGA GCA TC-3′ and R, 5′-ACA AGT ACA TCT CAG AGA TA-3′; At5g15600 F, 5′-ATG GGG AAA GCT AGA GGA GTT-3′ and R, 5′-TCA TTT GTC AGA TCC ACA AGG-3′; At5g15610 F, 5′-CCT CTT CAA TCT ATA TAA TCT-3′ and R, 5′-CTG AAA TAT ACT GGG AGC CTT-3′). The amplified fragments were cloned into the pGEM-T easy vector.

For RT-PCR analysis, *Arabidopsis* plants were grown on 1/2 MS medium and total RNA was extracted from 23-day-old plants using the total RNA Isolation System (Qiagen). RT-PCR was performed with the Access RT-PCR System (Invitrogen), according to the manufacturer's protocol. Briefly, 5 μg tRNA was reverse-transcribed to cDNA, diluted tenfold and amplified with the following specific primers: *LNG1* F, 5′-ATG TCG GCG AAG CTT TTG TAT A-3′ and R, 5′-GTC TCT TTC AAC TTG GCC CCT G-3′; *LNG2* F, 5′-CGA CTT GAG GAG TCT AAG GTC-3′ and R, 5′-GGA TCC CTG ATA ACC TTA AAA AAA TTA G-3′; actin (control) F, 5′-ATG ACT CAA ATC ATG TTT GAG ACC TTC-3′ and R, 5′-ACC TTA ATC TTC ATG CTG CTT GGA GC-3′; AN F, 5′-TGA GAC GGT GCC GTG GTA TGG-3′ and R, 5′-GTT GCC TAC TGG TGG ATT CC-3′; *ROT3F*, 5′-TGA GGC CTC GGT TGT TCT CA-3′ and *ROT3R*, 5′-TCT CTA CGA TCT TTC CGC TG-3′; *ATHB13-550R*, 5′-TTC TGT TAC TGC AAG ATC CTT CAG T-3′; *ATHB13-1F*, 5′-ATG TCT TGT AAT AAT GGA ATG TC-3′; *CYP90D1-F*, 5′-GCA CAA GTT TTT GTC GGA ATC C-3′; *CYP90D1-R*, 5′-GTC GAT CAT ATT GTT AGC AAT C-3′.

Anatomical analysis

Samples for the anatomical analysis were examined as described by Tsukaya et al. (Tsukaya et al., 1993). All plants were grown under identical conditions. The fifth leaves were fixed overnight in FAA solution (5% acetic acid, 45% ethanol and 5% formaldehyde), dried under a vacuum for 20 minutes and dehydrated in a graded ethanol series (50, 60, 70, 80, 90, 95, 99 and 100%) at room temperature. The dehydrated samples were incubated at room temperature in 50% Tchnovit 7100 resin (Kulzer and Company) and 50% ethanol for 2 hours, and then in 100% resin overnight. The resin was hardened at room temperature and the resin-impregnated leaves were sectioned at 4 μm through the center of the broad blade for longitudinal sections and through the widest part of the blade for transverse sections. The slices were fixed to glass slides, dried at room temperature, stained with 0.1% Toluidine Blue in 0.1 M phosphate buffer (pH 7.0), and observed and photographed under a microscope.

RESULTS

The *lng1-1D* mutant has longer lateral organs in its aerial part

To identify new genetic components involved in leaf morphogenesis, we screened *Arabidopsis* activation-tagging lines and isolated a dominant mutant, which we named *lng1-1D*. Fig. 1A shows the overall morphology of a soil-grown *lng1-1D* mutant plant. A leaf-by-leaf comparison with wild-type plants showed that all leaves of *lng1-1D* were longer and slightly narrower than those of the wild type (Fig. 1B), mainly owing to elongated leaf blades and leaf petioles. In addition, the leaves of *lng1-1D* were more deeply serrated than those of the wild type; this exacerbated serrated phenotype was due to the protrusion of existing hydathodes rather than to an increase in the number of hydathodes (Fig. 1B, right panel). The elongated phenotype of *lng1-1D* was not restricted to the rosette leaves. As shown in Fig. 1C-F, other aerial parts showed elongated phenotypes, including the floral tissues, siliques, seeds and cotyledons. The hypocotyl length of *lng1-1D* plants was slightly increased compared with the wild type, but the lengths of stems and primary roots were unchanged (see Table S1 in the supplementary material).

For quantitative comparison, we measured the lengths of various organs and structures, including primary roots, hypocotyls, petioles, leaf blades, internodes, siliques and seeds. The fully expanded leaf blades of *lng1-1D* mutants were 43% greater in length, but 29%

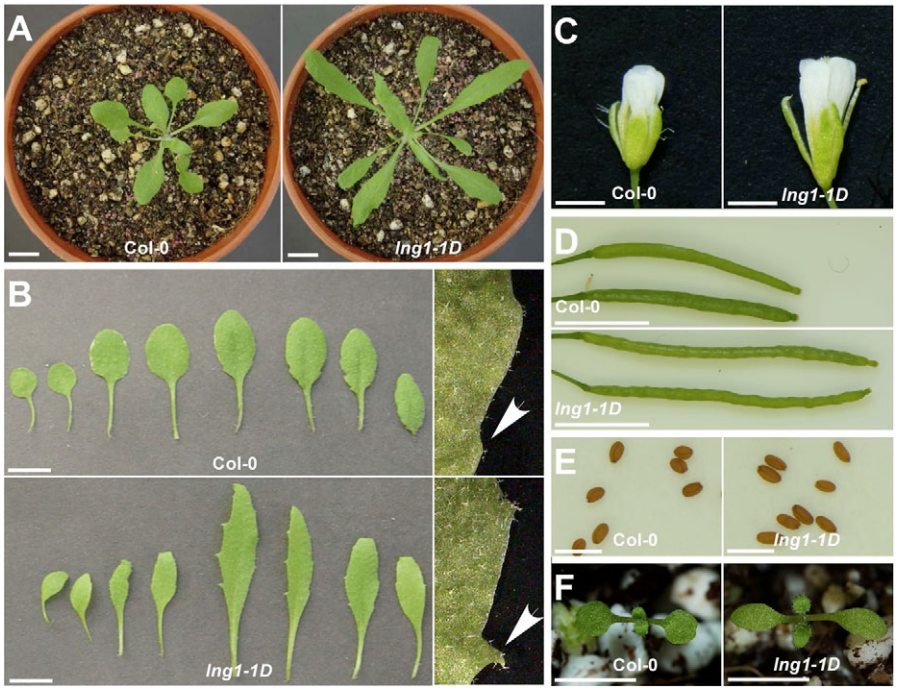

Fig. 1. The *lng1-1D* mutant shows long petioles, long leaves with serrated margins, long flowers and long siliques when compared with wild-type *Arabidopsis*. (**A**) 27-day-old wild-type and *lng1-1D* plants. (**B**) Rosette leaves of 39-day-old wild-type and *lng1-1D* plants. The right panels show magnified leaf margins and hydathodes of wild-type (top) and *lng1-1D* (bottom) plants. (C-E) Flowers (**C**), siliques (**D**), seeds (**E**) and cotyledons (**F**) of wild-type and *lng1-1D* plants. Scale bars: (A) 5 mm; (B) 10 mm; (C,E) 1 mm; (D,F) 2 mm.

narrower in width, compared with the wild type, suggesting that the mutation caused increased longitudinal leaf expansion with a concomitant decrease in transverse expansion (see Table S1 in the supplementary material). Consistent with the increased leaf length, the leaf petioles of *lng1-1D* mutants were 19% longer than those of the wild type, and the mutant seeds were longer (19%) and slightly narrower (6%) than those of wild type. Although there was no significant difference in stem length, the stem diameter was noticeably smaller (~25%) than that of wild-type plants. Taken together, the results indicated that the dominant *lng1-1D* mutation affects the longitudinal expansion of various parts of the plant, including the leaf blade, leaf petiole, flower, cotyledon and seed.

In *Arabidopsis*, the fifth leaf is regarded as a good representative of the rosette leaves (Tsuge et al., 1996). To investigate the kinetics of leaf expansion in the *lng1-1D* mutant, we monitored changes over time in the lengths and widths of fifth rosette leaf blades from at least 15 plants grown in soil under identical environmental conditions. As shown in Fig. 2A, the expansion rate of leaf blade width was initially comparable between *lng1-1D* and wild-type plants, but decreased faster in the *lng1-1D* mutant, leading to narrower mature leaves in the mutant. By contrast, the expansion rate of leaf blade length was higher in the *lng1-1D* mutant from the beginning, resulting in a greater final length of *lng1-1D* leaf blades compared with wild type (Fig. 2B). Expansion of the fifth leaves stopped around 39 days after sowing, both in wild type and *lng1-1D* mutants, suggesting that the mutation altered the expansion rate but not the timing of expansion during leaf development.

lng1-1D plants have elongated cells in their leaves, petals and siliques

Leaf expansion is determined by cell proliferation and expansion. To investigate whether cell expansion was affected in the *lng1-1D* mutant, we subjected the fifth rosette leaves of mutant and wild-type plants to scanning electron microscopy (SEM). Magnification of the leaf midvein area revealed that the adaxial epidermal cells in the midveins and the epidermal cells of nearby midveins were longitudinally elongated in *lng1-1D* leaves compared with wild type (Fig. 3A,B,D,E). On the adaxial side of the leaf blade, the epidermal cells of the *lng1-1D* mutant plants were longitudinally elongated compared with the wild type (Fig. 3C,F). To semi-quantify differences in cell size, we measured the lengths and widths of more than 150 adaxial epidermal cells in mutant and wild-type plants. The wild-type and *lng1-1D* cells had lengths of 88.0±11.6 μm (six plants) and 132.6±19.1 μm (five plants), respectively, and widths of 83.0±7.4 μm (six plants) and 59.8±9.4 μm (five plants), respectively. The *lng1-1D* epidermal cells were 51% longer and 28% narrower than their wild-type counterparts, suggesting that the longer, narrower cells of the mutant largely accounted for the differences in leaf phenotype. Similarly, the adaxial epidermal cells in the both proximal and distal mutant petals were longitudinally elongated and transversely narrowed in the *lng1-1D* mutant compared with wild type (Fig. 3G,H,K,L), as were the cells of the siliques (Fig. 3I,J,M,N).

LNG1 and *LNG2* encode novel proteins that activate longitudinal plant organ expansion

We performed a plasmid rescue experiment to identify the gene responsible for the *lng1-1D* mutant phenotypes and identified a single T-DNA insertion at 5477 bp upstream of At5g15880 (Fig. 4A). Since the T-DNA used included multiple copies of the 35S enhancer element, we tested whether the insertion caused the increased expression of nearby genes. Northern blot analysis indicated that the expression of one gene (At5g15880) was higher in mutant plants compared with wild type (Fig. 4B). This gene encodes a 927 amino acid protein containing a putative nuclear localization signal. BLAST searching identified no homologous proteins with known function, but did identify one closely related *Arabidopsis* homolog (At3g02170, 63% identical) of unknown function and a few related proteins from *Arabidopsis* and rice (~22-27% identical; Fig. 4C). Based on the sequence similarity and our functional analysis, we designated At5g15580 as *LNG1* and At3g02170 as *LNG2*. Amino acid sequence alignment indicated that

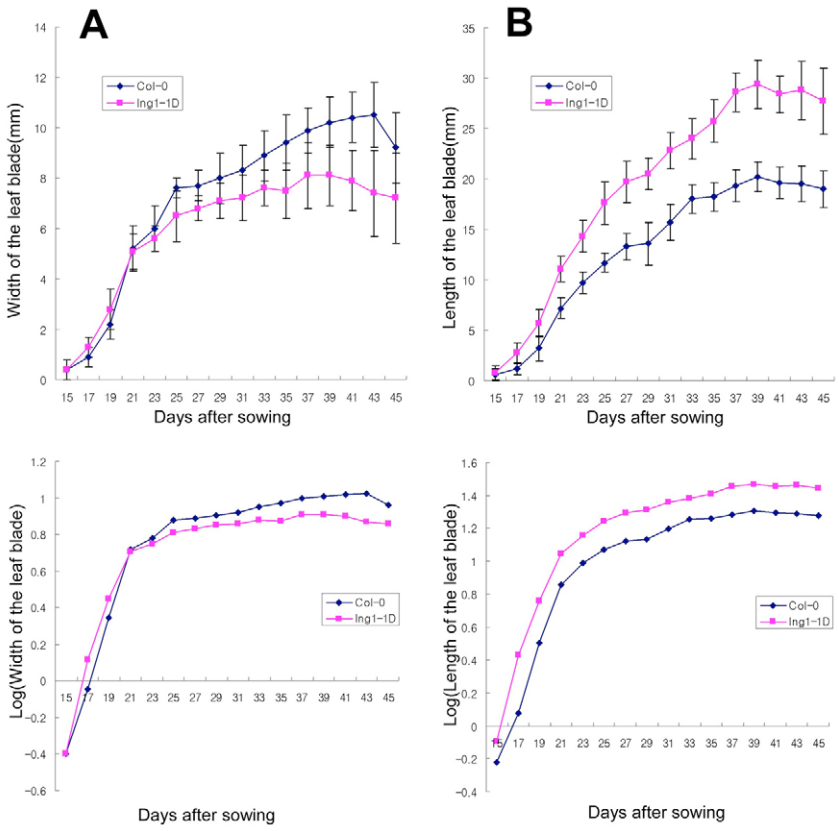

Fig. 2. Leaf growth of wild-type and *lng1-1D* mutant plants. (**A,B**) Measurement (top) and natural log (bottom) of the average width (A) and length (B) of 15 leaves of *lng1-1D* (squares) and wild type (diamonds).

several regions are well conserved among *LNG1*, *LNG2* and the related rice proteins (see Fig. S1 in the supplementary material). One of the conserved regions is serine rich, but none shows any similarity to known motifs.

To determine whether the elongated phenotypes of *lng1-1D* mutant plants were caused by the increased expression of *LNG1*, we generated transgenic *Arabidopsis* plants expressing this gene under the control of the CAMV 35S promoter. Similar to the phenotypes seen in the *lng1-1D* mutant, seven out of 15 independent transgenic lines displayed longer leaf blades, longer petioles and serrated leaf margins (Fig. 4F), indicating that overexpression of *LNG1* is responsible for the elongated phenotypes of the *lng1-1D* mutant. As *LNG2* is closely related to *LNG1*, we further tested whether overexpression of *LNG2* could cause elongated phenotypes. As shown in Fig. 4G, five out of 18 independent transgenic plants overexpressing *LNG2* also had longer petioles and slightly longer leaf blades. Interestingly, none of the *LNG2* overexpression lines had serrated leaves, suggesting that *LNG1* and *LNG2* have distinct, but overlapping, functions. Collectively, these results indicate that LNG1 and LNG2 are involved in directing leaf morphology by activating longitudinal cell expansion.

As LNG proteins have not been characterized in previous studies, we experimentally determined the subcellular localization of LNG1 in transgenic *Arabidopsis* plants expressing a GFP-LNG1 fusion protein and in onion epidermis that had been bombarded with GFP-LNG1 fusion constructs. Bombardment with vectors encoding GFP alone caused green fluorescence in both the cytosol and nucleus (data not shown), with the nuclear localization likely to be due to the low molecular weight of GFP alone (von Arnim et al., 1998). The GFP-LNG1 fusion protein showed similar localizations in both the cytosol and nucleus (Fig. 5A-C). However, since the molecular weight of the fusion protein is 131 kDa, the nuclear localization of the fusion protein is likely to reflect the actual nuclear localization of LNG1 protein. To confirm this finding, we generated transgenic plants expressing GFP-LNG1 fusion proteins under the control of the CAMV 35S promoter. The transgenic plants showed phenotypes similar to those of the *lng1-1D* mutants, including very elongated and serrated leaves (data not shown), suggesting that the GFP-LNG1 fusion protein is functional. The GFP signal, however, was relatively weak and was detected only faintly in the root tip cells of transgenic plants (Fig. 5D-G). Consistent with the subcellular localization in bombarded onion epidermal cells, GFP signals were detected in both the cytosol and nucleus. It is, however, possible that the cytosolic GFP signals were the result of partially degraded GFP-LNG1 proteins.

To further investigate the physiological functions of *LNG1* and *LNG2*, we determined the expression patterns of these genes in promoter:*GUS* transgenic plants. Promoter sequences (~2 kb) from the *LNG1* and *LNG2* genes were used to drive expression of *GUS*. The Pro_{LNG1}*:GUS* and Pro_{LNG2}*:GUS* transgenes were expressed in various parts of adult transgenic plants, including the petioles, leaf blades, floral organs and roots (Fig. 6). In roots, GUS staining was mainly detected in the lateral roots. GUS was strongly expressed in and at the base of the petioles (Fig. 6B,F). In leaves, GUS staining was observed in all parts, with stronger staining in the veins (Fig. 6C,G). Consistent with these observations, microarray analysis data compiled in Genevestigator (https://www.genevestigator.ethz.ch/) also indicate that LNG1 and LNG2 are expressed widely in various organs. These results collectively suggest that *LNG1* and *LNG2* are expressed in various *Arabidopsis* tissues, where they appear to regulate cell elongation.

We then characterized T-DNA-inserted putative loss-of-function *LNG1* (*lng1-2* and *lng1-3*) and *LNG2* (*lng2-1* and *lng2-2*) mutants, which were obtained from the ABRC (*Arabidopsis* Biological

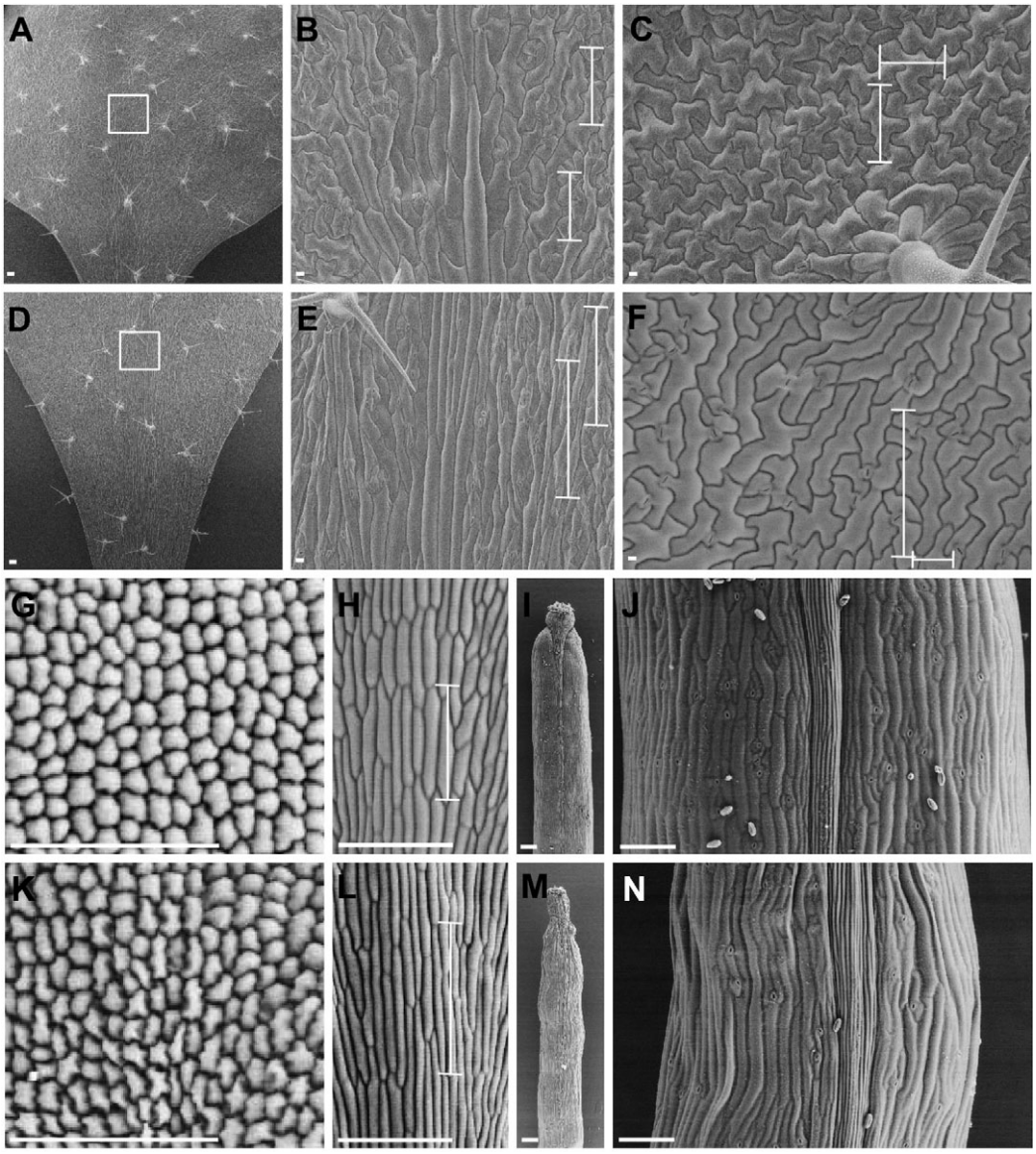

Fig. 3. Scanning electron microscope (SEM) analysis of epidermal cells. Wild-type Col-0 (**A-C**,**G-J**) and *lng1-1D* (**D-F**,**K-N**) plants at 27 (A-F) or 39 (G-N) days. The boxed regions in A and D are magnified in B and E. Bars in B and E indicate the length of a single cell. Scale bars: (A,D) 100 μm; (B,E) 20 μm. (C,F) Adaxial region of the fifth leaf. Scale bar: 10 μm. (G,K) The distal adaxial petal epidermis of wild-type (G) and *lng1-1D* (K) plants. Scale bar: 100 μm. (H,L) The proximal adaxial petal epidermis of wild-type (H) and *lng1-1D* (L) plants. The bar indicates the length of a single cell; scale bar: 20 μm. (I,J,M,N) The siliques of wild-type and *lng1-1D* plants. (J,N) Higher magnifications of I,M. Scale bars: (I,M) 200 μm; (J,N) 100 μm.

Resource Center; Fig. 7A). To determine whether the T-DNA insertion lines were true loss-of-function mutants, we tested their expression levels of *LNG1* and *LNG*. We observed weak expression of *LNG1* in *lng1-2* plants, but no such expression in *lng1-3*, indicating that *lng1-2* was a weak mutant allele and that *lng1-3* was a strong mutant allele (data not shown). No detectable expression of *LNG2* was observed in the *lng2-1* and *lng2-2* mutants, indicating that both *lng2-1* and *lng2-2* were strong mutant alleles. To determine whether *LNG1* and *LNG2* regulate each other, we examined the reciprocal expression levels in each line. As shown in Fig. 7B, loss-of-function of *LNG1* or *LNG2* did not affect the expression of the other gene. In addition, overexpression of *LNG1* (observed in the *lng1-1D* mutant) did not alter the expression of *LNG2*.

Next, we examined the phenotypes of the *lng1-3*, *lng2-1* and *lng1-3 lng2-1* loss-of-function mutants to determine the effects of LNG1 and LNG2 on various organs and structures. The lengths of cotyledons, rosette leaves, siliques and flowers were negligibly or only mildly affected in the *lng1-3* and *lng2-1* single mutant plants, but the *lng1-2 lng2-1* double mutant showed substantial decreases in the lengths of these organs (Fig. 7C). To quantify these differences, we measured various dimensions of these organs and structures in wild-type plants, as well as in *lng1-3*, *lng2-1* and *lng1-3 lng2-1* mutants (see Table S1 in the supplementary material). The widths of the leaf blades did not differ significantly among wild-type, *lng1-3*, *lng2-1* and *lng1-3 lng2-1* plants. By contrast, the leaf blade length was ~15% shorter in both single mutants, and almost 30% shorter in the double mutant, indicating that *LNG1* and *LNG2* additively regulate the leaf-length expansion. The additivity of *LNG1* and *LNG2* in leaf-length expansion was also observed in other organs. Petiole length did not significantly differ between the *lng1-3* and *lng2-1* single mutants and wild-type plants, but was 37% shorter in the double mutant compared with wild type. Similarly, the silique length of the double mutant was about 40% shorter (see Table S1 in the supplementary material; Fig. 7C). In addition to the decreased leaf-length expansion of these organs, we observed that the stem diameters of the double mutant plants were increased by almost 60% compared with the wild type. Taken together, these data suggest that *LNG1* and *LNG2* additively promote leaf-length expansion in various organs, while inhibiting the expansion of stem thickness.

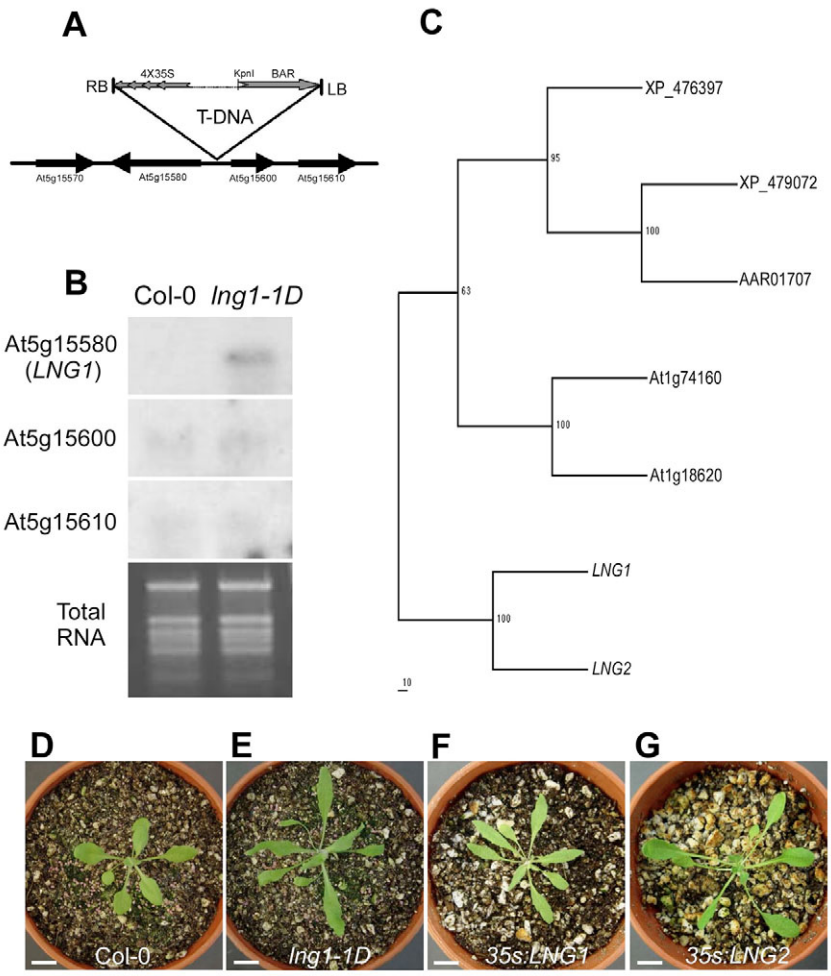

Fig. 4. The *lng1-1D* phenotype is caused by overexpression of *LNG1* (At5g15580). (**A**) Schematic representation of the T-DNA insertion site in the *lng1-1D* mutant. BAR, Basta resistance (Basta^r). 4×35S denotes four copies of the 35S enhancer. (**B**) Northern blot analysis of neighboring genes. The bottom panel shows total RNA. (**C**) *LNG1* and its homologs in *Arabidopsis* and rice. The unrooted phylogenetic tree was generated by a maximum parsimony method using the PHYLIP program. Numbers in the tree indicate bootstrap values. LNG1, At5g15580; LNG2, At3g02170; XP_476397, XP_479072 and AAR01707 include the *Oryza sativa*. (**D-G**) Recapitulation analysis with wild type (D), *lng1-1D* (E), 35S:*LNG1* (F) and 35S:*LNG2* (G). The plants were photographed 27 days after seeds were sown in the greenhouse.

LNG1 and LNG2 additively promote longitudinal polar cell elongation in the leaf

SEM analysis of *lng1-1D* mutant plants suggested that *LNG1* promotes longitudinal polar cell elongation. To further investigate the role of *LNG1* and *LNG2* in polar cell elongation, we determined cell sizes in transverse and longitudinal leaf sections (Table 1; see Fig. S2 in the supplementary material). In longitudinal sections, the palisade cells were 46% longer in the *lng1-1D* mutant than wild type, but 24% shorter in the *lng1-3 lng2-1* double mutant (Table 1; see Fig. S2 in the supplementary material). In transverse sections (representing width), however, we did not observe significant differences among the different lines (Table 1). Interestingly, cell proliferation did not appear to be significantly altered in the mutants. Both transverse and longitudinal sections showed similar numbers of palisade and mesophyll cells in wild-type, *lng1-1D*, *lng1-3*, *lng2-1* and *lng1-3 lng2-1* plants (Table 1). These results indicate that the altered leaf blade sizes in these plants are not due to altered cell proliferation, and that *LNG1* and *LNG2* regulate leaf expansion by promoting longitudinal polar cell elongation, not by regulating cell proliferation.

LNG1 and *LNG2* regulate longitudinal polar cell elongation independent of *ROT3*

Previous studies have shown that ROT3 regulates leaf expansion by promoting longitudinal cell expansion, not proliferation (Kim et al., 1998; Kim et al., 1999; Kim et al., 2002), whereas AN and ATHB13 regulate leaf expansion by promoting transverse cell expansion (Tsuge et al., 1996; Hanson et al., 2001; Kim et al., 2002). As our data indicate that cell expansion is also regulated by LNG1 and LNG2, we tested for functional relationships among these factors. We first tested for interrelation of their expression levels. Our results revealed that the expression levels of *ROT3*, *CYP90D1* (a *ROT3* homolog), *AN* and *ATHB13* were not altered in *lng1-1D* or *lng1-3 lng2-1* double mutant plants (Fig. 8A), and that *LNG1* and *LNG2* expression levels were unchanged in the *rot3-1* mutant (Fig. 8B), compared to wild type. These results indicate that *LNG1* and *LNG2* do not regulate expression of *ROT3*, *CYP90D1*, *AN* or *ATHB13*. Similarly, *ROT3* does not appear to regulate expression of *LNG1* or *LNG2*.

The functional relationship among these genes was further examined by analysis of a *lng1-3 lng2-1 rot3-1* triple mutant and of a *lng1-1D rot3-1* double mutant. The petiole length was shorter in the triple mutant compared with the *lng1-3 lng2-1* double mutant and *rot3-1* single mutant, both of which had shorter petioles than wild type (Fig. 8D). This difference in petiole length was mainly due to longitudinal shortening of the cells (see Table S2 in the supplementary material). By contrast, the leaf blade size of the triple mutant was similar to that of the *lng1-3 lng2-1* double mutant (Fig. 8C), and the blade cells were similar in size among the mutants (Fig. 8G; see Table S3 in the supplementary material). The leaf blades were already short in the *lng1-3 lng2-1* and *rot3-1* mutants, perhaps masking an additive shortening effect. Kozuka et al. suggested that

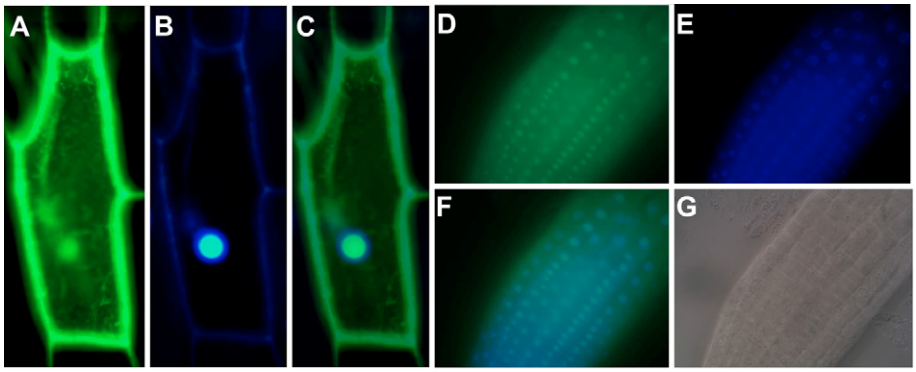

Fig. 5. Subcellular localization of LNG1-GFP fusion proteins. (**A-C**) Bombarded onion cells. (**D-G**) Transgenic *Arabidopsis* root. (A,D) GFP fluorescence. (B,E) Corresponding DAPI fluorescence. (C,F) Merged pictures. (G) Light microscopic picture of the corresponding cells.

the mechanism of petiole elongation differs from that of leaf blade elongation (Kozuka et al., 2005). Therefore, it is also possible that the LNG genes and *ROT3* may regulate petiole length additively, while regulating blade length in a collaborative fashion. To further clarify the relationships between *LNG1*, *LNG2* and *ROT3*, we measured the leaf blade length of an *lng1-1D rot3-1* double mutant. The blade lengths of *lng1-1D rot3-1* double mutant plants were intermediate between those of the *lng1-1D* overexpression line and the *rot3-1* loss-of-function mutant plants (Fig. 8C). The intermediate blade length of the *lng1-1D rot3-1* double mutant was due to cells of intermediate length, not to a change in cell number (Fig. 8G; see Table S3 in the supplementary material). Independent regulation of longitudinal elongation by LNG1 and ROT3 can also be seen in silique length (see Table S4 in the supplementary material). The *lng1-1D* had longer siliques than wild type, whereas the *lng1-3 lng2-1* double mutant and the *rot3-1* single mutant had shorter siliques. In support of independent regulation of longitudinal elongation by LNG1 and ROT3, the *lng1-3 lng2-1 rot3-1* triple mutant had even shorter siliques than the *lng1-3 lng2-1* double mutant or *rot3-1* single mutant, whereas the *lng1-1D rot3-1* double mutant had intermediate siliques compared with *lng1-1D* and *rot3-1* mutants. As *LNG1* does not regulate the expression of *ROT3* or of its close homolog *CYP90D1* (Fig. 8A), these results collectively suggest that *LNG1* and *ROT3* independently regulate longitudinal organ size (Fig. 8C-E).

The relationship between *LNG* and *ROT3* is less clear in terms of regulating leaf-width expansion. The *lng1-1D* mutant had a slightly narrower leaf blade compared with wild type, whereas the *rot3-1* mutant and the *lng1-1D rot3-1* double mutant showed similar phenotypes to each other, with a marginally wider leaf blade. The latter observation may suggest that *rot3-1* is epistatic to *lng1-1D* for leaf-width expansion. However, because the leaf blades of the *lng1-1D rot3-1* double mutants were shorter than those of the *lng1-1D* mutants, it is unclear whether the marginally wider leaf blade of the double mutant is caused by *rot3-1*, or is instead associated with the shortening of the leaf length.

Previous studies have shown that AN regulates transverse leaf expansion. To investigate whether LNG1 and AN themselves regulate longitudinal and transverse leaf expansion independently, we generated a *lng1-1D an* double mutant and examined leaf expansion. The *lng1-1D an* double mutants had longer petioles and longer leaf blades than wild-type plants (Fig. 8C,E). These results support the notion that longitudinal leaf expansion is regulated by LNG1 in an AN-independent fashion. For width direction, the relationship is not clear. The *lng1-1D an* double mutant had narrower leaf blades than wild type, but its widths were similar to those of the *an* single mutant. This suggests that *AN* is epistatic to *LNG1* for the width elongation of leaf blades. Alternatively, because the leaf blade of the *an* mutant is already narrow, it is possible that further narrowing in *lng1-1D an* double mutants was masked.

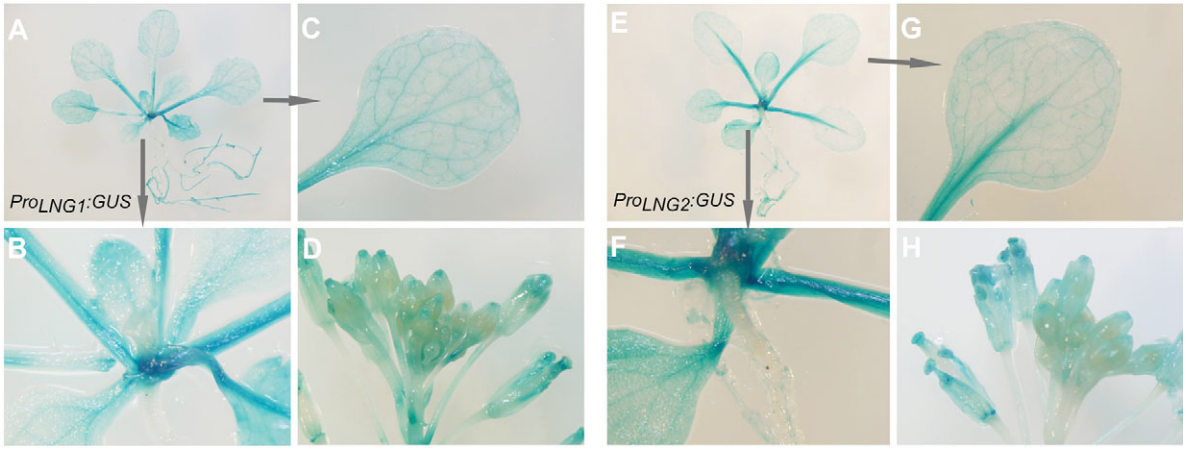

Fig. 6. Expression analysis of *Pro$_{LNG1}$:GUS* and *Pro$_{LNG2}$:GUS*. (**A-D**) X-Gluc staining of a 23-day-old *Pro$_{LNG1}$:GUS* transgenic plant (A-C), and of a flower cluster from a 6-week-old representative of the same transgenic line (D). (**E-H**) X-Gluc staining of a 23-day-old *Pro$_{LNG2}$:GUS* transgenic plant (E-G), and a flower cluster from a 6-week-old representative of the same transgenic line (H).

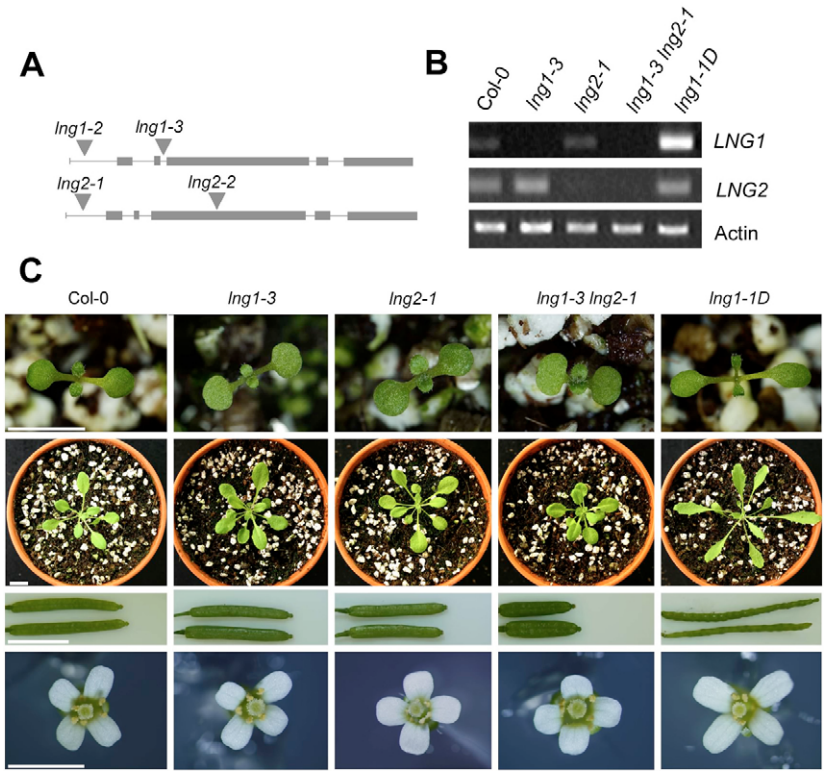

Fig. 7. *LNG1* and *LNG2* additively promote longitudinal organ elongation. (**A**) T-DNA insertion sites of the *lng1-2*, *lng1-3*, *lng2-1*, and *lng2-2* mutants. (**B**) Expression analysis of *LNG1* and *LNG2* in the wild type, *lng1-3*, *lng2-1*, *lng1-3 lng2-1*, and *lng1-1D* mutants. (**C**) Phenotypes of the wild type, *lng1-3*, *lng2-1*, *lng1-3 lng2-1*, and *lng1-1D* plants. Top panel, 8-day-old cotyledons. Scale bar: 5 mm. Second panel, 27-day-old plants. Scale bar: 10 mm. Third panel, siliques. Scale bar: 5 mm. Bottom panel, flowers. Scale bar: 5 mm.

To investigate whether LNG1 functions at a specific leaf developmental stage, we determined the cell numbers and cell sizes throughout the various leaf developmental stages. The cell numbers in the fifth leaf increased until 21 days after sowing, and no difference was observed between wild-type and mutant plants (Fig. 8F; see Table S3 in the supplementary material), indicating that cell numbers are not regulated by *LNG1*, *LNG2* or *ROT3*. The cell sizes increased longitudinally up to 39 days after sowing, both in wild-type and mutant plants (Fig. 8G), but the cell elongation rates of *lng1-1D* and *lng1-3 lng2-1* cells were higher and lower, respectively, than that of wild-type cells at all tested leaf developmental stages. Taken together, these results suggest that *LNG1*, *LNG2* and *ROT3* additively promote longitudinal cell expansion in petioles and leaf blades throughout leaf development, rather than increasing cell number or acting at a specific leaf developmental stage.

DISCUSSION

We report that the novel *Arabidopsis* genes *LNG1* and *LNG2* are responsible for regulating the expansion of various aerial parts, including leaves, flowers and siliques, by promoting longitudinal cell expansion at the expense of transverse cell expansion. Our genetic analysis reveals that *LNG1* and *LNG2* regulate longitudinal polar cell elongation independently of *ROT3*, suggesting that *Arabidopsis* contains at least two independent pathways for promoting longitudinal cell expansion.

LNG1 and *LNG2* promote longitudinal polar cell elongation in a *ROT3*-independent fashion

Characterization of a dominant *Arabidopsis* mutant with unusually long petioles, leaves, petals and siliques allowed us to identify a gene involved in longitudinal expansion of aerial plant organs. We

Table 1. Measurement of the cell number and cell size in the fifth leaf of wild-type and mutant plants

	Col-0	*lng1-1D*	*lng1-3*	*lng2-1*	*lng1-3 lng2-1*
Number of cells counted in the longitudinal sections (leaf-length direction)					
Palisade cells	384.2±35.9 (*n*=5)	395.9±60.0 (*n*=5)	348.4±40.7 (*n*=5)	388.3±16.2 (*n*=6)	383.6±69.0 (*n*=5)
Mesophyll cells	976.4±108.9 (*n*=5)	1033.2±170.0 (*n*=5)	890.2±112.6 (*n*=5)	998.3±112.9 (*n*=6)	1017.8±98.6 (*n*=5)
Half number of cells in the transverse sections (leaf-width direction)					
Palisade cells	113.0±12.5 (*n*=6)	116.4±17.3 (*n*=5)	108.2±7.7 (*n*=5)	116.2±9.2 (*n*=6)	116.7±14.3 (*n*=6)
Mesophyll cells	307.2±26.9 (*n*=6)	347.0±45.0 (*n*=5)	281.4±33.4 (*n*=5)	341.0±14.2 (*n*=6)	302.5±21.4 (*n*=6)
Palisade cell size (μm)					
Leaf-length direction (*n*=5)	47.9±5.2	69.8±4.6*	47.4±7.9	40.8±5.4	36.5±3.7*
Leaf-width direction (*n*=5)	41.5±6.1	36.4±2.3	41.1±4.6	45.2±5.2	45.7±3.2
Leaf thickness in the length direction (*n*=5)	45.6±7.9	39.6±1.8	47.6±6.7	47.7±5.6	51.7±2.0

Fully expanded leaves from 39-day-old plants were measured in longitudinal and transverse sections. For cell size measurements, more than 200 cells were examined per section. *n*, number of plant leaves measured for cell number. Results are shown ±s.d.
*Compared with the wild type, level of significance was 5% (paired Student's *t*-test).

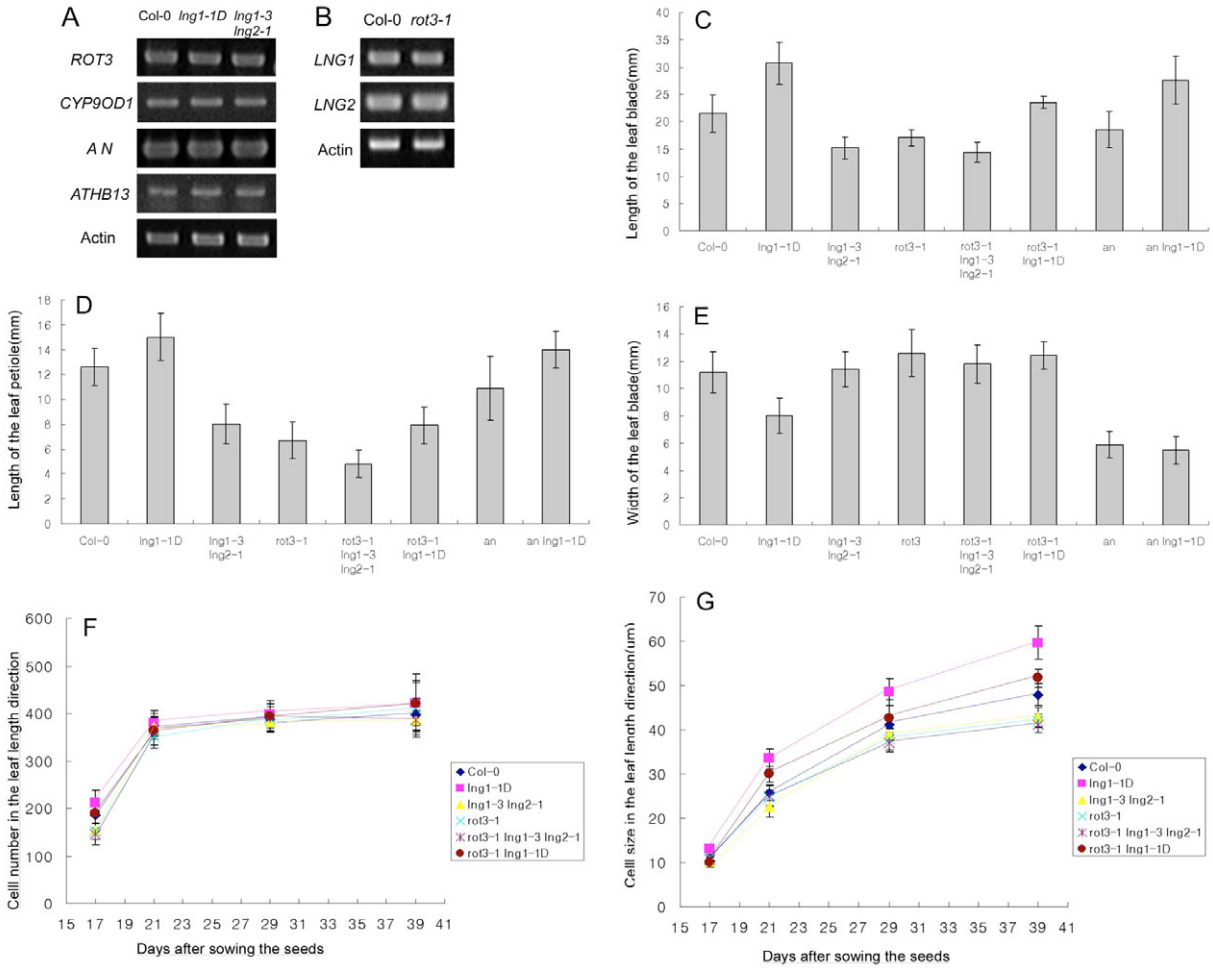

Fig. 8. *LNG1* and *LNG2* regulate longitudinal cell expansion independently of *ROT3*. (**A**) RT-PCR expression analysis of *ROT3, CYP90D1, AN and ATHB13* in wild-type, *lng1-1D* and *lng1-3 lng2-1* plants. (**B**) Expression analysis of *LNG1* and *LNG2* in wild-type and *rot3-1* plants. (**C**) Length of the leaf blade. (**D**) Length of the leaf petiole. (**E**) Width of the leaf blade. Analyses were performed on the fifth leaves of 39-day-old plants. Measurement of cell numbers (**F**) and cell sizes (**G**) of the fifth leaves during different developmental stages. Paradermal images of palisade cells were used for measurements.

designated this gene *LNG1* and identified a homolog in *Arabidopsis*, which we designated *LNG2*. *LNG1* and *LNG2* play positive roles in longitudinal organ expansion in length direction, as evidenced by the elongated organs of the *lng1-1D* mutant and transgenic lines overexpressing *LNG1* or *LNG2* (Fig. 4F,G), or the shortened organs of plants harboring loss-of-function mutations in *LNG1* and *LNG2*. Consistent with their amino acid sequence similarity (63%), analysis of the *lng1 lng2* double loss-of-function mutant revealed that *LNG1* and *LNG2* are functionally overlapping genes.

Paradermal and section image analysis of leaf blade cells showed that the cell numbers in the leaf blades were almost identical between wild-type and mutant/transgenic lines, suggesting that *LNG1* and *LNG2* do not affect cell proliferation (Table 1, see Fig. S2 and Table S3 in the supplementary material). However, the same analysis indicated that cells were lengthened in the *lng1-1D* plants, and additively shortened in *lng1-3 lng2-1* double mutants in the leaf-length direction. The ratio of wild-type to mutant cell length was roughly equivalent to the ratio of wild-type to mutant leaf length. Taken together, these results indicate that *LNG1* and *LNG2* regulate organ expansion by regulating polar cell elongation, not cell proliferation.

The roles of *LNG1* and *LNG2* in longitudinal cell expansion appear similar to that of the previously characterized *ROT3*. For example, *ROT3*-overexpression lines have longer leaf cells compared with the wild type (Kim et al., 1999), whereas *rot3-1* loss-of-function mutants have shorter organs comprising shorter cells (Tsuge et al., 1996). Although these similar phenotypes could indicate that these genes are members of the same pathway, several lines of evidence suggest that *LNG1* and *LNG2* regulate longitudinal cell expansion independently of *ROT3*. First, our expression analysis revealed that altering the expression levels of *LNG1* and *LNG2* did not alter the expression levels of *ROT3* or its homolog, *CYP90D1* (Fig. 8A). Second, the *lng1-3 lng2-1 rot3-1* triple loss-of-function mutant showed additive shortening of cell length, whereas the *lng1-1D rot3-1* double mutant showed an intermediate cell length, particularly in the case of petiole cells (see Table S2 in the supplementary material). Third, the *lng1-1D rot3-1* double mutant showed longer leaf blades and petioles compared with the *rot3-1* single mutant, but shorter leaf blades and petioles compared with the *lng1-1D* single mutant. These data indicate that the two classes of genes do not have an epistatic relationship with regard to longitudinal cell expansion, suggesting that longitudinal cell expansion is regulated by at least two

independent pathways in *Arabidopsis*: one involving *ROT3*, and the other involving *LNG1* and *LNG2*. As *ROT3* encodes an enzyme required for BR biosynthesis (Kim et al., 2005), these data further suggest that *Arabidopsis* contains a BR-independent pathway that regulates longitudinal polar cell elongation.

The novel proteins LNG1 and LNG2 have homologs in other plant species

Analysis of the predicted protein sequences of LNG1 and LNG2 indicated that they are novel proteins of unknown function. However, BLAST analysis identified homologous protein sequences in *Arabidopsis* and rice. The *Arabidopsis* genome contains two additional LNG-like proteins showing overall sequence similarity and a few proteins that show partial sequence similarity. In rice, we identified three proteins showing ~22-27% overall sequence similarity to LNG1 (Fig. 4C; see Fig. S1 in the supplementary material). Multiple sequence alignment of the four *Arabidopsis* proteins and the three rice proteins allowed us to identify several regions that are well conserved among the family members. One conserved region is highly enriched with serine residues, but overall these regions overall lack known motifs. Taken together, these results suggest that LNG family members are novel plant-specific proteins that promote longitudinal polar cell elongation through unknown mechanisms.

The presence of LNG-like genes in other plant species raises the possibility that these genes might play important roles in shaping various plant forms. In *Arabidopsis*, different ecotypes display different leaf shapes, ranging from *rot3*-like round leaves to *an*-like narrow leaves. Previous QTL analysis using recombinant inbred lines identified 21 QTL responsible for the natural variations found in adult leaves of the Ler and Col-4 ecotypes (Perez-Perez et al., 2002). Notably, one of the reported QTL loci (ad-LSI2) overlaps with the chromosome position of *LNG1*. According to the QTL analysis, ad-LSI2 was responsible for about 5% of the variance found in the recombinant inbred lines. Further experiments are needed to prove that *LNG1* corresponds to ad-LSI2.

This work was supported, in part, by grants from KOSEF (R21-2003-000-1002-0), the Agricultural Plant Stress Research Center (R11-2001-092-01002-0) and the Plant Metabolism Research Center (R11-2000-081), and by a MOST/KOSEF grant from the Environmental Biotechnology National Core Research Center (R15-2003-002-01002-0). We also thank the Korea Basic Science Institute (KBSI) for assistance with the Scanning Electron Microscope (SEM) analysis.

Supplementary material

Supplementary material for this article is available at
http://dev.biologists.org/cgi/content/full/133/21/4305/DC1

References

Altmann, T. (1998). Recent advances in brassinosteroid molecular genetics. *Curr. Opin. Plant Biol.* **1**, 378-383.

Azpiroz, R., Wu, Y., LoCascio, J. C. and Feldmann, K. A. (1998). An Arabidopsis brassinosteroid-dependent mutant is blocked in cell elongation. *Plant Cell* **10**, 219-230.

Berna, G., Robles, P. and Micol, J. L. (1999). A mutational analysis of leaf morphogenesis in *Arabidopsis thaliana*. *Genetics* **152**, 729-742.

Bowman, J. L., Eshed, Y. and Baum, S. F. (2002). Establishment of the polarity in angiosperm lateral organs. *Trends Genet.* **18**, 134-141.

Choe, S., Dilkes, B. P., Fujioka, S., Takatsuto, S., Sakurai, A. and Feldmann, K. A. (1998). The DWF4 gene of Arabidopsis encodes a cytochrome P450 that mediates multiple 22alpha-hydroxylation steps in brassinosteroid biosynthesis. *Plant Cell* **10**, 231-243.

Clough, S. J. and Bent, A. F. (1998). Floral dip: a simplified method for *Agrobacterium*-mediated transformation of *Arabidopsis thaliana*. *Plant J.* **16**, 735-743.

De Veylder, L., Beeckman, T., Beemster, G. T., Krols, L., Terras, F., Landrieu, I., van der Schueren, E., Maes, S., Naudts, M. and Inze, D. (2001). Functional analysis of cyclin-dependent kinase inhibitors of Arabidopsis. *Plant Cell* **13**, 1653-1668.

Franklin, K. A., Davis, S. J., Stoddart, W. M., Vierstra, R. D. and Whitelam, G. C. (2003). Mutant analyses define multiple roles for phytochrome C in Arabidopsis photomorphogenesis. *Plant Cell* **15**, 1981-1989.

Fujioka, S., Li, J., Choi, Y. H., Seto, H., Takatsuto, S., Noguchi, T., Watanabe, T., Kuriyama, H., Yokota, T., Chory, J. et al. (1997). The Arabidopsis deetiolated2 mutant is blocked early in brassinosteroid biosynthesis. *Plant Cell* **9**, 1951-1962.

Hanson, J., Johannesson, H. and Engstrom, P. (2001). Sugar-dependent alterations in cotyledon and leaf development in transgenic plants expressing the HDZhdip gene ATHB13. *Plant Mol. Biol.* **45**, 247-262.

Hemerly, A., Engler Jde, A., Bergounioux, C., Van Montagu, M., Engler, G., Inze, D. and Ferreira, P. (1995). Dominant negative mutants of the Cdc2 kinase uncouple cell division from iterative plant development. *EMBO J.* **15**, 3925-3936.

Jones, A. M., Im, K. H., Savka, M. A., Wu, M. J., DeWitt, N. G., Shillito, R. and Binns, A. N. (1998). Auxin-dependent cell expansion mediated by overexpressed auxin-binding protein 1. *Science* **6**, 1114-1117.

Kim, G. T. and Cho, K. H. (2006). Recent advances in the genetic regulation of the shape of simple leaves. *Physiol. Plantarum* **126**, 494-502.

Kim, G. T., Tsukaya, H. and Uchimiya, H. (1998). The *ROTUNDIFOLIA3* gene of *Arabidopsis thaliana* encodes a new member of the cytochrome P-450 family that is required for the regulated polar elongation of leaf cells. *Genes Dev.* **12**, 2381-2391.

Kim, G. T., Tsukaya, H., Saito, Y. and Uchimiya, H. (1999). Changes in the shapes of leaves and flowers upon overexpression of cytochrome P450 in Arabidopsis. *Proc. Natl. Acad. Sci. USA* **96**, 9433-9437.

Kim, G. T., Shoda, K., Tsuge, T., Cho, K. H., Uchimiya, H., Yokoyama, R., Nishitani, K. and Tsukaya, H. (2002). The *ANGUSTIFOLIA* gene of Arabidopsis, a plant CtBP gene, regulates leaf-cell expansion, the arrangement of cortical microtubules in leaf cells and expression of a gene involved in cell-wall formation. *EMBO J.* **21**, 1267-1279.

Kim, G. T., Fujioka, S., Kozuka, T., Tax, F. E., Takatsuto, S., Yoshida, S. and Tsukaya, H. (2005). CYP90C1 and CYP90D1 are involved in different steps in the brassinosteroid biosynthesis pathway in *Arabidopsis thaliana*. *Plant J.* **41**, 710-721.

Kozuka, T., Horiguchi, G., Kim, G. T., Ohgishi, M., Sakai, T. and Tsukaya, H. (2005). The different growth responses of the *Arabidopsis thaliana* leaf blade and the petiole during shade avoidance are regulated by photoreceptors and sugar. *Plant Cell Physiol.* **46**, 213-223.

Li, J. and Chory, J. (1997). A putative leucine-rich repeat receptor kinase involved in brassinosteroid signal transduction. *Cell* **90**, 929-938.

Narita, N. N., Moore, S., Horiguchi, G., Kubo, M., Demura, T., Fukuda, H., Goodrich, J. and Tsukaya, H. (2004). Overexpression of a novel small peptide *ROTUNDIFOLIA4* decreases cell proliferation and alters leaf shape in *Arabidopsis thaliana*. *Plant J.* **38**, 699-713.

Perez-Perez, J. M., Serrano-Cartagena, J. and Micol, J. L. (2002). Genetic analysis of natural variations in the architecture of *Arabidopsis thaliana* vegetative leaves. *Genetics* **162**, 893-915.

Qin, M., Kuhn, R., Moran, S. and Quail, P. H. (1997). Overexpressed phytochrome C has similar photosensory specificity to phytochrome B but a distinctive capacity to enhance primary leaf expansion. *Plant J.* **12**, 1163-1172.

Sinha, N. (1999). Leaf development in angiosperms. *Annu. Rev. Plant Physiol. Plant Mol. Biol.* **50**, 419-446.

Timpte, C. C., Wilson, A. K. and Estelle, M. (1992). Effects of the *axr2* mutation of Arabidopsis on cell shape in hypocotyl and inflorescence. *Planta* **188**, 271-278.

Tsuge, T., Tsukaya, H. and Uchimiya, H. (1996). Two independent and polarized processes of cell elongation regulate leaf blade expansion in *Arabidopsis thaliana* (L.) Heynh. *Development* **122**, 1589-1600.

Tsukaya, H. (2003). Organ shape and size: a lesson from studies of leaf morphogenesis. *Curr. Opin. Plant Biol.* **6**, 57-62.

Tsukaya, H., Naito, S., Rédei, G. P. and Komeda, Y. (1993). A new class of mutations in *Arabidopsis thaliana, acaulis1,* affecting the development of both inflorescences and leaves. *Development* **118**, 751-764.

Ullah, H., Chen, J. G., Young, J. C., Im, K. H., Sussman, M. R. and Jones, A. M. (2001). Modulation of cell proliferation by heterotrimeric G protein in Arabidopsis. *Science* **15**, 2066-2069.

Verkest, A., Manes, C. L., Vercruysse, S., Maes, S., Van Der Schueren, E., Beeckman, T., Genschik, P., Kuiper, M., Inze, D. and De Veylder, L. (2005). The cyclin-dependent kinase inhibitor KRP2 controls the onset of the endoreduplication cycle during Arabidopsis leaf development through inhibition of mitotic CDKA;1 kinase complexes. *Plant Cell* **17**, 1723-1736.

von Arnim, A. G., Deng, X. W. and Stacey, M. G. (1998). Cloning vectors for the expression of green fluorescent protein fusion proteins in transgenic plants. *Gene* **221**, 35-43.

Wang, H., Zhou, Y., Gilmer, S., Whitwill, S. and Fowke, L. C. (2000). Expression of the plant cyclin-dependent kinase inhibitor ICK1 affects cell division, plant growth and morphology. *Plant J.* **24**, 613-623.

Weigel, D., Ahn, J. H., Blazquez, M. A., Borevitz, J. O., Christensen, S. K., Fankhauser, C., Ferrandiz, C., Kardailsky, I., Malancharuvil, E. J., Neff, M. M. et al. (2000). Activation tagging in Arabidopsis. *Plant Physiol.* **122**, 1003-1013.